GEOPHYSICAL RESEARCH LETTERS, VOL. ???, XXXX, DOI:10.1029/,

Submitted 17 October 2011 to Geophysical Research Letters, resubmitted in revised form 15 November 2011, accepted 16 November 2011.

How pore fluid pressurization influences crack tip processes during dynamic rupture

Nicolas Brantut,[1,2,3] and James R. Rice[3]

We calculate temperature and pore pressure rises along a steadily propagating shear crack, assuming a given shear stress profile along the crack (i.e., initially neglecting effects of pore pressure on shear stress). In the limit of a singular crack, temperature and pore pressure rises are a step function in time. We verify that pore pressure can indeed be neglected at the tip and in the cohesive zone of the crack in the case of strong velocity weakening of the friction coefficient (e.g., as governed by flash heating of asperities, like analyzed in a recent numerical simulation of spontaneous rupture). In such cases, the local fracture energy needed to increase the crack length is thus likely to be governed by "dry" frictional processes with effective slip weakening distance of the order of 20 μm, while thermal pressurization may affect the later stages of slip and hence the overall fracture energy attributed to the propagating rupture.

1. Introduction

Earthquakes propagate because the fault rocks lose strength as slip occurs. Studies on rock friction generally show that the ratio of shear stress to normal stress must be of the order of 0.6 to 0.8 to initiate slip [*Byerlee*, 1978]. At slip rates of the order of 1 m/s, the ratio of shear stress to normal stress diminishes dramatically with increasing slip, down to 0.2 or 0.1. This drop can be attributed to various mechanisms, most of them being thermally based [*Di Toro et al.*, 2011]. A distinction can be made between mechanisms active in dry or unsaturated rocks, and those occurring only in fluid saturated rocks. A number of "dry" frictional weakening processes have been recognized, such as flash heating [e.g., *Rice*, 2006], silica gel formation [*Goldsby and Tullis*, 2002; *Di Toro et al.*, 2004], dehydration and amorphization [*Hirose and Bystricky*, 2007; *Brantut et al.*, 2008], thermal decomposition [*Han et al.*, 2007, 2010], and melting [e.g., *Hirose and Shimamoto*, 2005]. In fluid saturated rocks, thermal pressurization of pore fluid is an important weakening mechanism [e.g., *Lachenbruch*, 1980; *Andrews*, 2002; *Bizzarri and Cocco*, 2006a, b; *Rice*, 2006].

A way to understand the controlling factors in the weakening behaviour of fault rocks is to compare the rise time (or characteristic slip distance) of thermal pressurization to the characteristic activation time (or slip) of any of the "dry" weakening mechanism depicted above. In particular, flash heating is activated at slip rates of the order of 0.1m s^{-1}, and associated with characteristic slip weakening distance of the order of the asperities' size, from 1 to 25 μm or less [*Goldsby and Tullis*, 2011]. Hence, weakening by flash heating is likely to be the first and dominant weakening process at early times during fault slip [see *Noda et al.*, 2009, for an in-depth discussion]. For constant slip rates of the order of 1 m/s, the characteristic slip weakening distance determined from thermal pressurization is usually of the order of a few centimeters [e.g., *Noda and Shimamoto*, 2005], i.e., much larger than the slip needed to induce flash heating. However, the slip rate during dynamic ruptures is far from being constant: for instance, during the propagation of a singular crack-like rupture, the slip rate is theoretically infinite at the tip and decays as the inverse of the square root of time as slip proceeds. Recently *Noda et al.* [2009] studied dynamic rupture processes by performing elastodynamic simulations including (1) flash heating (embedded in a rate-and-state framework) and (2) thermal pressurization. However, it is still unclear at which stage each of those processes is dominant.

Here we aim at estimating the pore pressure evolution during ruptures with realistic slip history, and determine at which stage does pore fluid pressurization significantly affect the mechanics of the fault. First, we use a simplified slip-weakening description of the rupture tip breakdown process to extract the slip rate history. Then, we compute pore pressure and temperature rises due to thermal pressurization, and estimate in which conditions the pore pressure rise can be neglected. We finally compare our simplified results to the full elastodynamic simulations performed by *Noda et al.* [2009].

2. Slip Weakening Mechanism and Crack Tip Description

2.1. Weakening by Flash Heating

Recent studies [e.g., *Di Toro et al.*, 2011] suggest that the intrinsic friction coefficient of rocks decreases dramatically from around 0.8 down to 0.1 or less during fault motion at coseismic slip rates, independently from macroscopic pore fluid pressurization effects. One of the mechanism suggested to explain this decrease in friction is flash heating at asperity contacts [*Rice*, 1999, 2006; *Beeler et al.*, 2008; *Goldsby and Tullis*, 2011]: During sliding at high slip rate, the local temperature increase induced by shear heating on slip surface asperities can lead to thermal weakening (e.g., melting or thermal decomposition) of those asperities, which leads to a macroscopic decrease in friction. A constitutive friction law accounting for flash heating has been described by *Noda et al.* [2009]. Since weakening by flash heating was originally described for uniform slip rate, and is a velocity-weakening process, *Noda et al.* [2009] regularized their friction law by incorporating direct effect and state evolution, which ensured well-posedness of the elastodynamic frictional sliding problem [*Rice et al.*, 2001]. As a result, the model provided

[1]Rock and Ice Physics Laboratory, Department of Earth Sciences, University College London, London, UK.
[2]Laboratoire de Géologie, CNRS UMR 8538, École Normale Supérieure, Paris, France.
[3]Department of Earth and Planetary Sciences and Division of Engineering and Applied Sciences, Harvard University, Cambridge, Massachusetts, USA.

0094-8276/11/$5.00

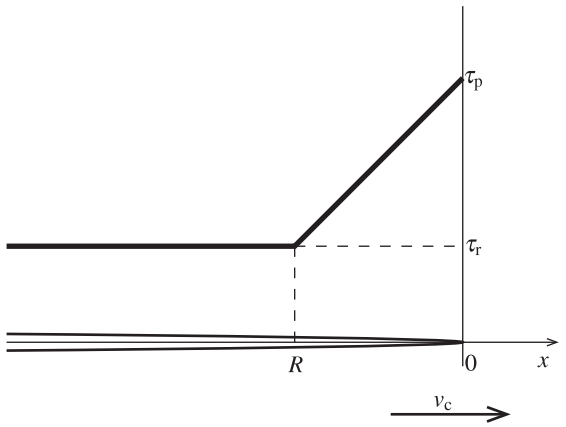

Figure 1. Cohesive zone model at the rupture tip. Stress linearly decreases with increasing distance to the tip. The rupture is propagating at constant velocity v_c.

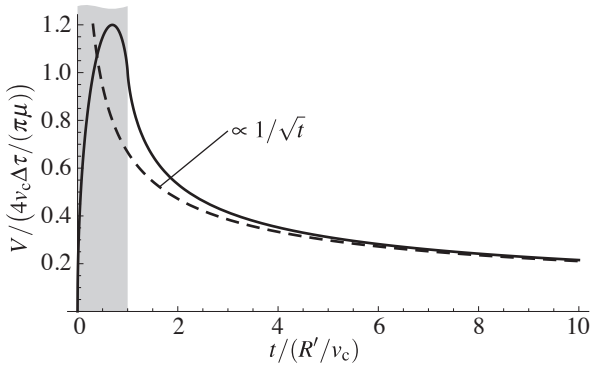

Figure 2. Normalized slip rate history obtained from the cohesive zone model (equation 8). The cohesive zone corresponds to the shaded area. Away from it, the slip rate decreases as $1/\sqrt{t}$, which corresponds to a singular crack.

by *Noda et al.* [2009] is of the form

$$f = a\ln(V/V_0) + \Theta, \tag{1}$$

$$\frac{d\Theta}{dt} = -\frac{V}{L}[f - f_{ss}], \tag{2}$$

where V is the sliding velocity, $a = 0.016$ is the nondimensional direct effect, V_0 is a reference velocity, Θ is the state variable (as defined by *Nakatani* [2001]), L is the state evolution distance and f_{ss} is a steady-state friction coefficient for sustained sliding at a uniform slip rate equal to the momentary V. At the onset of a dynamic rupture, the abrupt increase in slip rate from $V_0 \sim 10^{-6}$ m/s to $V \sim 1$ m/s induces a short term increase in friction coefficient of $a\ln(10^6) \sim 0.22$. Using an initial friction coefficient of ~ 0.6, the expected peak friction is then $f_p = 0.82$. On the other hand, at high velocity ($V \gtrsim 1$ m/s), the new steady-state friction f_{ss} is low due to weakening by flash heating and *Noda et al.* [2009] provide the value $f_{ss} = f_w = 0.13$. The evolution from f_p to f_w is achieved over a slip distance of the order of L. The friction law can thus be usefully simplified as

$$\frac{df}{dt} = -\frac{V}{L}[f - f_w], \quad f(t=0) = f_p. \tag{3}$$

Integrating, we obtain $f = f_w + (f_p - f_w)\exp(-\delta/L)$, where δ is the slip. This is merely a slip weakening description of friction, and L is now equivalent to a slip-weakening distance. In such a framework, assuming a constant effective normal stress σ' on the fault, we can calculate the fracture energy G:

$$G = \int [\tau(\delta) - \tau_r]d\delta = \int \sigma'[f(\delta) - f_w]d\delta = (f_p - f_w)L\sigma'. \tag{4}$$

Using an effective normal stress of $\sigma' = 126$ MPa, representative of the ambient Terzaghi effective pressure at 7 km depth, and a length $L = 20\,\mu m$ commensurable with asperity size [*Noda et al.*, 2009], which L we adopt to be consistent with their study, the fracture energy associated with that near-tip weakening is around $G = 1.7$ kJ/m^2.

2.2. Cohesive Zone Model and Slip Rate History

Based on the above considerations, and still neglecting pore fluid pressurization, we describe the displacement and shear strength evolution at a rupture tip using the slip weakening model of *Palmer and Rice* [1973]. The shear stress is written as (see Figure 1):

$$\tau = \begin{cases} (\tau_p - \tau_r)x/R + \tau_r & 0 \le x < R, \\ \tau_r & R \le x, \end{cases} \tag{5}$$

where $\tau_p = f_p\sigma'$ is the peak stress, $\tau_r = f_w\sigma'$ is the residual stress, x is the coordinate along the crack, with the tip momentarily at $x = 0$, and R is the cohesive zone length. given (in mode III, antiplane slip) by

$$R = \frac{9\pi}{16}\frac{\mu G}{(\tau_p - \tau_r)^2}, \tag{6}$$

where μ is the shear modulus of the fault rock. The expression 6 holds for a quasi-static crack under remote driving stress τ_∞, with $\tau_\infty - \tau_r \ll \tau_p - \tau_r$, and must be modified as $R' = R/g_{III}(v_c)$ when the rupture is propagating dynamically [*Rice*, 1980]. The function g_{III} of crack velocity v_c is given by

$$g_{III}(v_c) = \frac{1}{\sqrt{1 - v_c^2/c_s^2}}, \tag{7}$$

where c_s is the shear wave velocity of the surrounding medium. For a moving crack at constant speed v_c, the slip rate $V(t)$ is extracted from the slip distribution behind the tip $\delta(x)$ (given in *Palmer and Rice* [1973]) as $V(t) = -v_c\partial\delta/\partial x$ for $x = -v_c t$. We thus obtain, in mode III,

$$V(t) = \frac{2}{\pi}\frac{\tau_p - \tau_r}{\mu}\left(2\sqrt{\frac{v_c t}{R'}} + \left(1 - \frac{v_c t}{R'}\right)\ln\left|\frac{1 + \sqrt{v_c t/R'}}{1 - \sqrt{v_c t/R'}}\right|\right). \tag{8}$$

A similar expression holds in mode II, with g_{III} replaced by an analogue function g_{II} of the rupture speed and μ replaced by $\mu/(1-\nu)$ where ν is the Poisson's ratio of the rock [*Rice*, 1980]. Figure 2 shows the slip rate normalized by $v_c 4(\tau_p - \tau_r)/(\pi\mu)$ as a function of normalized time $t/(R'/v_c)$. In the limit of vanishingly small cohesive zone length ($R' \to 0$), or far away from the cohesive zone, the model is that of a singular crack and the slip rate becomes (see dotted line in Figure 2)

$$V(t) \sim 2\sqrt{\frac{Gv_c}{\pi\mu g_{III}(v_c)t}} \propto 1/\sqrt{t}. \tag{9}$$

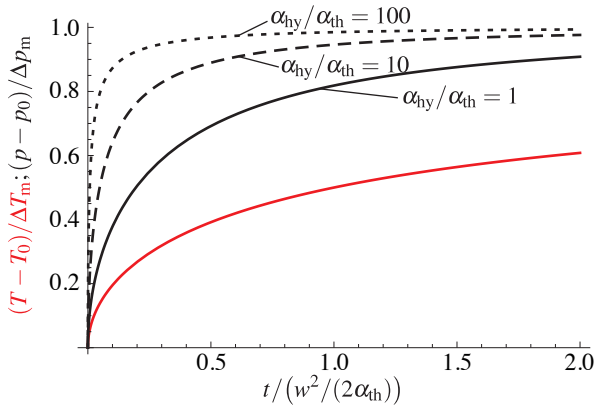

Figure 3. Normalized pore pressure (black) and temperature (red) changes as a function of normalized time for a rupture with vanishingly small cohesive zone length. The steady-state pore pressure is reached more rapidly for high hydraulic diffusivity. For negligibly small thickness w, the changes are step functions in time.

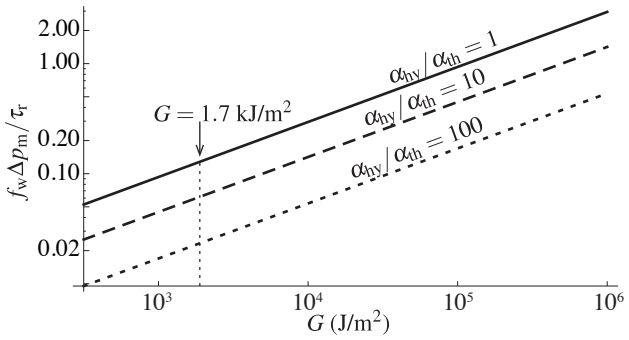

Figure 4. Ratio of the pore pressure effect on shear stress over the assumed constant residual shear stress as a function of fracture energy, for various hydraulic diffusivities. The other parameter values are $\alpha_{th} = 0.7$ mm^2/s, $\Lambda = 0.47$ MPa/°C, $\mu = 30$ GPa, $c_s = 3$ km/s and $v_c = 0.8c_s$. For the fracture energy calculated from the flash heating weakening mechanism (1.7 kJ/m^2), the maximum effect of pore pressure on shear stress remains low compared to the assumed residual stress.

Relations 8 and 9 provide realistic slip rate histories expected from a linear strength drop behind the crack tip. They hold for crack-like rupture, and are also valid solutions near the propagating front for self-healing pulses in the limit case of very small static stress drop compared to strength drop and very large rupture length compared to cohesive zone length [*Rice et al.*, 2005].

3. Thermal Pressurization of Pore Fluid

In the previous section we described the strength evolution at the crack tip "dry" frictional processes only, and assuming constant pore fluid pressure. The consistency of this assumption can be tested by calculating the temperature and pore pressure rises along the crack tip due to shear heating and thermal pressurization of pore fluid.

3.1. Governing Equations

The conservation of energy and fluid mass provides a coupled system of differential equations that governs the temperature (denoted T) and pore pressure (denoted p) evolution [e.g., *Andrews*, 2002; *Rice*, 2006]:

$$\frac{\partial T}{\partial t} = \alpha_{th}\frac{\partial^2 T}{\partial y^2} + \frac{\omega(y,t)}{\rho c}, \tag{10}$$

$$\frac{\partial p}{\partial t} = \alpha_{hy}\frac{\partial^2 p}{\partial y^2} + \Lambda\frac{\partial T}{\partial t}, \tag{11}$$

where y is the coordinate normal to the rupture plane, α_{th} and α_{hy} are respectively thermal and hydraulic diffusivities, ρc is the specific heat of the rock, Λ is the pore pressure change per unit temperature change under undrained conditions, and $\omega(y,t)$ is the heat source due to shear dissipation. The porosity is considered constant: the effect of dilatancy at the onset of slip would be a limitation of the pore pressure changes [*Garagash and Rudnicki*, 2003]. Hence the assumption of constant porosity yields an upper bound for the pore pressure rise. Here we assume a Gaussian distribution of shear strain rate across the fault, over a root-mean-square half-width w. The heat source is thus

$$\omega(y,t) = \frac{\tau(t)V(t)}{w\sqrt{2\pi}}\exp\left(-\frac{y^2}{2w^2}\right). \tag{12}$$

The solution for temperature and pore pressure is then [*Rice*, 2006, Appendix B]

$$T(y,t) = T_0 + \frac{1}{\rho c}\int_0^t \tau(t')V(t')A(y,t-t';\alpha_{th})dt', \tag{13}$$

$$p(y,t) = p_0 + \frac{\Lambda}{\rho c}\int_0^t \tau(t')V(t') \cdot \left[\frac{\alpha_{th}A(y,t-t';\alpha_{th}) - \alpha_{hy}A(y,t-t';\alpha_{hy})}{\alpha_{th} - \alpha_{hy}}\right]dt', \tag{14}$$

where T_0 and p_0 are the initial (ambient) temperature and pore pressure, respectively, and

$$A(y,t;\alpha) = \frac{1}{\sqrt{2\pi(w^2 + 2\alpha t)}}\exp\left(-\frac{y^2}{2(w^2 + 2\alpha t)}\right). \tag{15}$$

3.2. Singular Crack Limit

In the approximation of negligibly small cohesive zone length, we have seen (equation 9) that the slip rate decreases as $1/\sqrt{t}$ while the applied shear stress remains constant at its residual value $\tau(t) = \tau_r$. In that case, the integrals 13 and 14 can be carried out analytically at $y = 0$, and give the following solutions for temperature and pore pressure at the center line of the shearing zone:

$$T(0,t) = T_0 + \Delta T_m \frac{2}{\pi}\arcsin\left[\frac{1}{\sqrt{1 + w^2/(2\alpha_{th}t)}}\right], \tag{16}$$

$$p(0,t) = p_0 + \Delta p_m \frac{2}{\pi}\left(\sqrt{\alpha_{th}}\arcsin\left[\frac{1}{\sqrt{1 + w^2/(2\alpha_{th}t)}}\right] - \sqrt{\alpha_{hy}}\arcsin\left[\frac{1}{\sqrt{1 + w^2/(2\alpha_{hy}t)}}\right]\right)/(\sqrt{\alpha_{th}} - \sqrt{\alpha_{hy}}), \tag{17}$$

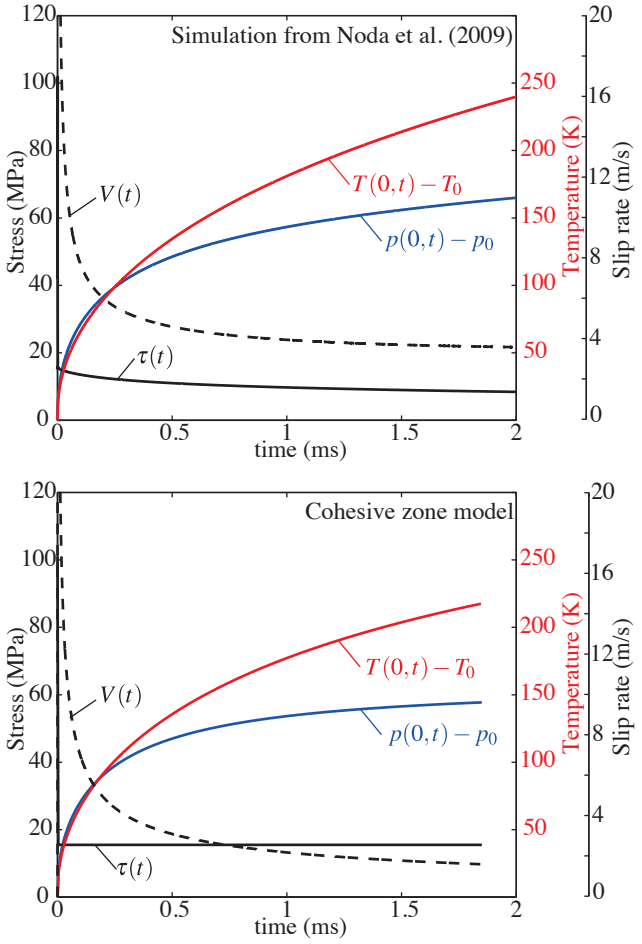

Figure 5. Comparison between the elastodynamic simulation of a crack-like rupture from *Noda et al.* [2009] (top) and the simplified cohesive model with assumed constant residual stress (bottom) using the same parameter values.

where

$$\Delta T_{\rm m} = \frac{\tau_{\rm r}}{\rho c}\sqrt{\frac{\pi G v_{\rm c}}{2\alpha_{\rm th}\mu g_{\rm III}(v_{\rm c})}}, \tag{18}$$

$$\Delta p_{\rm m} = \Lambda\frac{\sqrt{\alpha_{\rm th}}}{\sqrt{\alpha_{\rm th}}-\sqrt{\alpha_{\rm hy}}}\Delta T_{\rm m}, \tag{19}$$

are the maximum temperature and pore pressure changes. Figure 3 is a normalized plot of the temperature and pore pressure increases as a function of normalized time $2\alpha_{\rm th}t/w^2$. The maximum, steady-state pore pressure is reached all the more rapidly than the ratio of hydraulic and thermal diffusivities is large. Remarkably, for vanishingly small thickness of the fault ($w \to 0$), the pore pressure and temperature rise instantaneously up to their maximum values and then remain constant. This rather surprising feature had already been noticed by *Andrews* [2002], and is explained by the fact that the temperature on the plane would increase as $\sqrt{t}$ for a constant heat source, while heat is supplied on the plane as $1/\sqrt{t}$. In the slip on a plane approximation, we retrieve the proportionality between p and T (equation 19) noted by *Rice* [2006], and thus the same argument holds for the pore pressure rise.

Our hypothesis of constant residual shear stress will be proved wrong if the change in shear stress due to pore pressure, i.e., $f_{\rm w}(p-p_0)$, becomes significant compared to $\tau_{\rm r}$. A conservative estimate of the relative importance of pore pressure compared to residual stress is given by the ratio

$$\frac{f_{\rm w}\Delta p_{\rm m}}{\tau_{\rm r}} = \frac{f_{\rm w}\Lambda}{\rho c}\frac{1}{\sqrt{\alpha_{\rm th}}+\sqrt{\alpha_{\rm hy}}}\sqrt{\frac{\pi G v_{\rm c}}{2\mu g_{\rm III}(v_{\rm c})}}. \tag{20}$$

Figure 4 is a plot of the ratio 20 as a function of fracture energy G, for parameter values $\alpha_{\rm th} = 0.7$ mm^2/s, $\Lambda = 0.47$ MPa/°C, $\mu = 30$ GPa, $c_{\rm s} = 3$ km/s and $v_{\rm c} = 0.8c_{\rm s}$. Even for low hydraulic diffusivity $\alpha_{\rm hy} \approx \alpha_{\rm th} = 0.7$ mm^2/s, the fracture energy $G = 1.7$ kJ/m^2 calculated from the flash heating mechanism implies a negligible pore pressure effect on shear stress compared to the total residual shear stress, i.e., $f_{\rm w}\Delta p_{\rm m}/\tau_{\rm r} \lesssim 0.1$. For fracture energies greater than 10 kJ/m^2 and hydraulic diffusivities of the order of 1 mm^2/s, the maximum pore pressure rise induces a non negligible effect on the residual shear stress. In this case, the rise time of the pore pressure rise is approximately given by $w^2/(2\alpha_{\rm hy})$. For $w = 0.1$ mm and $\alpha_{\rm hy} = 1$ mm^2/s, this rise time is of the order of 0.05 s. The rupture speed being of the order of 3 km/s, a significant increase in pore pressure would occur at around 15 m from the rupture tip. If $w = 1$ mm, the same increase occurs at around 1.5 km from the rupture tip. Thus, for thick slipping zones (of the order of a few mm), thermal pressurization of pore fluid affects shear stress on the fault only at later stage during slip and not close to the rupture front.

3.3. Finite Cohesive Zone Length

Let us now consider a cohesive zone of finite length. In that case, the temperature and pore pressure given in equations 13 and 14 have to be evaluated numerically. The integrals are calculated using Matlab's QUADGK integration routine. By using the parameter values given by *Noda et al.* [2009] in our simplified semi-analytical model, we can try to reproduce some of their results, which were produced by full elastodynamic simulations. The only unknown parameter is $v_{\rm c}$, which is adjusted manually to fit the peak slip rate of the simulation. A value of $v_{\rm c} = 0.999c_{\rm s}$ produces a reasonable reproduction of the simulated slip rate. Figure 5 shows a comparison plot for a crack-like rupture simulated by *Noda et al.* [2009, their Figure 7b and 7d]. The simplified slip-weakening model reproduces reasonably well the pore pressure and temperature rises. At lower rupture speeds the expected p and T changes are significantly lower and occur on longer timescales (see Figure S1). As expected, the shear stress in overestimated by the simplified model since the pore pressure rise is not taken into account. As a result, the slip rate is not perfectly matched over long times, and is underestimated by the simplified model.

4. Discussion and Conclusion

In the framework of frictional heating by flash heating of asperity contacts, we have seen that it is legitimate to neglect the additional weakening due to pore fluid pressurization close to the rupture tip. However, judging from the scaling depicted in Figure 4, this justification does not hold for fracture energies larger than a few kJ/m^2. For a given friction drop, the fracture energy depends on the effective normal stress and the slip-weakening distance (equation 4). The effective normal stress is dictated by the depth and the ambient pore pressure; however, very little constrains exist on the weakening distance. In the case of flash heating,

Noda et al. [2009] argue that L should be at maximum of the order of the asperity size, i.e., a few tens of micrometers at most. An independent constrain can be attempted by extrapolation of high velocity friction experiments data. *Brantut et al.* [2008] suggested that the slip weakening distance at high slip rates should scale with the inverse of the square of the normal stress applied to the fault. Thus, weakening distances of the order of 1 m at around 1 MPa [e.g., *Mizoguchi et al.*, 2007] turn into a few hundreds of microns (or less) at mid-seismogenic depth (around 100 MPa effective normal stress). On the other hand, *Di Toro et al.* [2011] described empirical power law dependence of slip weakening distance on normal stress, which yields extrapolated values of the order of a few millimeters (for fault gouges materials) at seismogenic depth. From these extrapolations, we expect a local fracture energy of the order of 10 to 100 kJ/m^2. In this range of fracture energies, the effect of pore pressure rise on shear stress is not always negligible (see Figure 4), but the finiteness of the slipping zone width delays the pore pressure increase. The effect of pore pressure on shear stress is thus important only after the rupture tip has passed in the fault rock. In any event, as confirmed by the comparison of the simplified model with dynamic simulations, the pore pressure rise is not expected to alter significantly the shear stress evolution within the cohesive zone close to the crack tip.

An important implication is that the weakening arising from the flash heating process, operating even in dry conditions, is controlling the local fracture energy and cohesive zone width. As mentioned earlier, pore fluid pressurization becomes important beyond the cohesive zone associated with onset of flash weakening of the crack. Thus, the apparent fracture energy that would be computed using the entire stress-displacement curve, like calculated approximately [*Rice*, 2006] in the case of slip at a uniform 1 m/s rate, would also include an important contribution from thermal pressurization. The estimates of the local fracture energy from the weakening by flash heating, of the order of a few kJ m^{-2}, can thus be much lower than the global seismological estimates which are of the order of several MJ m^{-2} for $M_{\rm w}7$ earthquakes [e.g., *Mai et al.*, 2006]. However, we have shown here that this apparent "long term" contribution does not necessary imply an actual contribution to the cohesive zone weakening processes.

A limitation of our study is that an elastic response off the fault has been assumed. At rupture speeds close to the the S-wave speed, off-fault yielding will tend to increase the fracture energy and possibly the cohesive zone length as the rupture propagates [*Andrews*, 2005]. Thus, for long ruptures (the length of which yet remains to be determined by numerical simulations), fluid pressurization will become more and more significant even within the cohesive zone. Precise estimations of such effects yet remain to be determined by numerical simulations. A subtlety in using relation 4 is that the fracture energy, even in the case of purely elastic behavior off the fault plane, is well defined (see derivations in *Palmer and Rice* [1973] and *Rice* [1980]) only when the shear stress on the rupture plane reaches a constant residual value $\tau_{\rm r}$ over most of that plane. Thus, we have made a consistent definition of G for the portion of rupture very near the tip using $\tau_{\rm r} = f_{\rm w}\sigma'$ with σ' based on the ambient pore pressure, assumed to not yet be eroded by thermal pressurization over the small distance scales of order R' involved. Using that $G = f_{\rm w}\sigma' L$ to set the strength of an equivalent elastic singularity, we could bypass the resolution of the small-scale details of strength evolution during onset of flash weakening and just use $f_{\rm w}\sigma'$ as the shear traction at the tip of the slipping zone of a singular crack. However, if we considered far greater distances from the tip, but still small compared to overall rupture length, and assumed that thermal pressurization had there reduced σ' to 0, then the only valid choice for calculating G for the overall rupture from relation 4 would be to use $\tau_{\rm r} = 0$.

Acknowledgments. This work has been supported by the Geomechanics Research Fund at Harvard and by the Southern California Earthquake Center (SCEC) funded by NSF Cooperative Agreement EAR-0529922 and USGS Cooperative Agreement 07HQAG0008. The SCEC contribution number for this paper is xxxx. We have benefited from discussions with John Platt and Robert Viesca, and simulation data were kindly provided by Eric Dunham and Hiroyuki Noda.

References

Andrews, D. J., A fault constitutive relation accounting for thermal pressurization of pore fluid, *J. Geophys. Res.*, *107*(B12), 2363, doi:10.1029/2002JB001942, 2002.

Andrews, D. J., Rupture dynamics with energy loss outside the slip zone, *J. Geophys. Res.*, *110*, B01307, doi:10.1029/2004JB003191, 2005.

Beeler, N. M., T. E. Tullis, and D. L. Goldsby, Constitutive relationships and physical basis of fault strength due to flash heating, *J. Geophys. Res.*, *113*, B01401, doi:10.1029/2007JB004988, 2008.

Bizzarri, A., and M. Cocco, A thermal pressurization model for the spontaneous dynamic rupture propagation on a threedimensional fault: 1. Methodological approach, *J. Geophys. Res.*, *111*, B05303, doi:10.1029/2005JB003862, 2006a.

Bizzarri, A., and M. Cocco, A thermal pressurization model for the spontaneous dynamic rupture propagation on a threedimensional fault: 2. Traction evolution and dynamic parameters, *J. Geophys. Res.*, *111*, B05304, doi:10.1029/2005JB003864, 2006b.

Brantut, N., A. Schubnel, J.-N. Rouzaud, F. Brunet, and T. Shimamoto, High velocity frictional properties of a clay-bearing fault gouge and implications for earthquake mechanics, *J. Geophys. Res.*, *113*, B10401, doi:10.1029/2007JB005551, 2008.

Byerlee, J. D., Friction of rocks, *Pure Appl. Geophys.*, *116*, 615–626, 1978.

Di Toro, G., D. Goldsby, and T. E. Tullis, Friction falls towards zero in quartz rock as slip velocity approaches seismic rates, *Nature*, *427*, 436–439, 2004.

Di Toro, G., R. Han, T. Hirose, N. De Paola, S. N. K. Mizoguchi, F. Ferri, M. Cocco, and T. Shimamoto, Fault lubrication during earthquakes, *Nature*, *471*, 494–498, 2011.

Garagash, D. I., and J. W. Rudnicki, Shear heating of a fluid-saturated slip-weakening dilatant fault zone 1. limiting regimes, *J. Geophys. Res.*, *108*(B2), 2121, doi:10.1029/2001JB001653, 2003.

Goldsby, D. L., and T. E. Tullis, Low frictional strength of quartz rocks at subseismic slip rates, *Geophys. Res. Lett.*, *29*(17), 1844, doi:10.1029/2002GL015240, 2002.

Goldsby, D. L., and T. E. Tullis, Flash heating leads to low frictional strength of crustal rocks at earthquake slip rates, *Science*, *334*, 216–218, 2011.

Han, R., T. Shimamoto, T. Hirose, J. Ree, and J. Ando, Ultra-low friction of carbonate faults caused by thermal decomposition, *Science*, *316*(5826), 878–881, 2007.

Han, R., T. Hirose, and T. Shimamoto, Strong velocity weakening and powder lubrication of simulated carbonate faults at seismic slip rates, *J. Geophys. Res.*, *115*, B03412, doi:10.1029/2008JB006136, 2010.

Hirose, T., and M. Bystricky, Extreme dynamic weakening of faults during dehydration by coseismic shear heating, *Geophys. Res. Lett.*, *34*, L14311, doi:10.1029/2007GL030049, 2007.

Hirose, T., and T. Shimamoto, Growth of molten zone as a mechanism of slip weakening of simulated faults in gabbro during frictional melting, *J. Geophys. Res.*, *110*, B05202, doi:10.1029/2004JB003207, 2005.

Lachenbruch, A. H., Frictional heating, fluid pressure, and the resistance to fault motion, *J. Geophys. Res.*, *85*, 6097–6122, 1980.

Mai, P. M., P. Somerville, A. Pitarka, L. Dalguer, S. Song, G. Beroza, H. Miyake, and K. Irikura, On scaling of fracture energy and stress drop in dynamic rupture models: Consequences for near-source ground-motions, in *Earthquakes: radiated energy and the physics of faulting*, edited by R. Abercrombie, A. McGarr, G. Di Toro, and H. Kanamori, Geophys. Monogr. Ser., American Geophysical Union, Washington, DC, 2006.

Mizoguchi, K., T. Hirose, T. Shimamoto, and E. Fukuyama, Reconstruction of seismic faulting by high-velocity friction experiments: An example of the 1995 Kobe earthquake, *Geophys. Res. Lett.*, *34*, L01308, doi:10.1029/2006GL027931, 2007.

Nakatani, M., Conceptual and physical clarification of rate and state friction: Frictional sliding as a thermally activated rheology, *J. Geophys. Res.*, *106*(B7), 13,347–13,380, 2001.

Noda, H., and T. Shimamoto, Thermal pressurization and slip-weakening distance of a fault: An example of Hanaore fault, southwest Japan, *Bull. Seism. Soc. Am.*, *95*(4), 1224–1233, 2005.

Noda, H., E. M. Dunham, and J. R. Rice, Earthquake ruptures with thermal weakening and the operation of major faults at low overall stress levels, *J. Geophys. Res.*, *114*, B07302, doi: 10.1029/2008JB006143, 2009.

Palmer, A. C., and J. R. Rice, The growth of slip surfaces in the progressive failure of over-consolidated clay, *Proc. Roy. Soc. Lond. A.*, *332*, 527–548, 1973.

Rice, J. R., The mechanics of earthquake rupture, in *Physics of the Earth's Interior*, edited by A. M. Dziewonski and E. Boschi, Proc. Intl. School of Physics E. Fermi, Italian Physical Society/North Holland Publ. Co., 1980.

Rice, J. R., Flash heating at asperity contacts and rate-depend friction, *Eos. Trans. AGU*, *80*(46), Fall Meet. Suppl., 1999.

Rice, J. R., Heating and weakening of faults during earthquake slip, *J. Geophys. Res.*, *111*, B05311, doi: 10.1029/2005JB004006, 2006.

Rice, J. R., N. Lapusta, and K. Ranjith, Rate and state dependent friction and the stability of sliding between elastically deformable solids, *J. Mech. Phys. Solids*, *49*, 1865–1898, 2001.

Rice, J. R., C. G. Sammis, and R. Parsons, Off-fault secondary failure induced by a dynamic slip pulse, *Bull. Seism. Soc. Am.*, *95*(1), 109–134, 2005.

N. Brantut, Rock and Ice Physics Laboratory, Department of Earth Science, University College London, Gower Street, London WC1E 6BT, UK. (nicolas.brantut@normalesup.org)

J. R. Rice, Department of Earth and Planetary Sciences and School of Engineering and Applied Sciences, Harvard University, 224 Pierce Hall, 29 Oxford Street, Cambridge, MA 02138, USA. (rice@seas.harvard.edu)